

# Supplementary Materials for Fast-MVSNet: Sparse-to-Dense Multi-View Stereo With Learned Propagation and Gauss-Newton Refinement

Zehao Yu  
ShanghaiTech University  
yuzh@shanghaitech.edu.cn

Shenghua Gao  
ShanghaiTech University  
gaoshh@shanghaitech.edu.cn

## 1. Architecture

As presented in the main paper, our Fast-MVSNet has three parts: sparse high-resolution depth map prediction, depth map propagation, and Gauss-Newton refinement. For the sparse high-resolution depth map prediction, our network is similar to MVSNet [4] except that we build a sparse cost volume in spatial domain and use fewer virtual depth planes (e.g., 96). Therefore, we can obtain a sparse high-resolution depth map at much lower cost. For the depth map propagation module, we use a 10-layer convolutional network to prediction the weights  $W$ . We show the details of this network in Table 1. For the Gauss-Newton refinement, we use a similar network architecture as propagation module to extract deep feature representations of the input images  $\{I_i\}_{i=0}^N$ . In particular, Conv\_4 and Conv\_7 as in Table 1 are first interpolated to the same size and then are concatenated as the deep feature representation.

Name	Layer	Output Size
Input		$H \times W \times 3$
Conv_0	ConvBR, K=3x3, S=1, F=8	$H \times W \times 8$
Conv_1	ConvBR, K=3x3, S=1, F=8	$H \times W \times 8$
Conv_2	ConvBR, K=5x5, S=2, F=16	$\frac{1}{2}H \times \frac{1}{2}W \times 16$
Conv_3	ConvBR, K=3x3, S=1, F=16	$\frac{1}{2}H \times \frac{1}{2}W \times 16$
Conv_4	ConvBR, K=3x3, S=1, F=16	$\frac{1}{2}H \times \frac{1}{2}W \times 16$
Conv_5	ConvBR, K=5x5, S=2, F=32	$\frac{1}{4}H \times \frac{1}{4}W \times 32$
Conv_6	ConvBR, K=3x3, S=1, F=32	$\frac{1}{4}H \times \frac{1}{4}W \times 32$
Conv_7	Conv, K=3x3, S=1, F=32	$\frac{1}{4}H \times \frac{1}{4}W \times 32$
Conv_8	Conv, K=3x3, S=1, F=16	$\frac{1}{4}H \times \frac{1}{4}W \times 16$
$W$	Conv, K=3x3, S=1, F= $k^2$	$\frac{1}{4}H \times \frac{1}{4}W \times k^2$

Table 1: Weights prediction network in the propagation module. We denote the 2D convolution as Conv and use BR to abbreviate the batch normalization and the Relu. K is the kernel size, S the kernel stride and F the output channel number. H, W denote image height and width, respectively.

## 2. Depth maps fusion

The fusion has three steps: photometric filtering, geometric consistency, and depth fusion. For photometric filtering, we first interpolate the predicted probability of the sparse high-resolution depth map to a high-resolution probability map and filter out points whose probability is below a threshold. The filtering threshold is set to 0.5. For geometric consistency, we compute the discrepancy of each depth map and filter out points whose discrepancy is larger than a threshold  $\eta$ . Specifically, a point  $p$  in reference depth map  $D$  is first projected to  $p'$  in the neighboring depth map  $\hat{D}$ , then the discrepancy is defined as  $f \cdot baseline \cdot \left\| \frac{1}{D(p)} - \frac{1}{\hat{D}(p')} \right\|$ , where  $f$  is the focal length of reference image and  $baseline$  is the baseline of two images. The threshold  $\eta$  is set to 0.12 pixels. For depth fusion, we require each point to be visible in  $V = 3$  views and take the average value of all reprojected depths.

In the main paper, for a fair comparison, we use the same parameters for depth map fusion as that in Point-MVSNet [2]. However, we find that the fusion parameters  $\eta$  and  $V$  have a significant impact on reconstruction results. We show the quantitative comparison of reconstructions with different  $\eta$  and  $V$  in Table 2. The comparison of visualization results are shown in Figure 1. From the comparison results, we can see the trade off between *Accuracy* and *Completeness*. Increasing  $\eta$ , the reconstructed points gets less accurate but more complete. Increasing  $V$ , the reconstructions become more accurate while become incomplete. As the fusion has significant impact on the final reconstruction results, integrating a learnable fusion module [3] into the overall pipeline will be an interesting direction in future work.

## 3. Gauss-Newton refinement with more iterations

In this section, we conduct ablation study for Gauss-Newton refinement with more iterations. As shown in

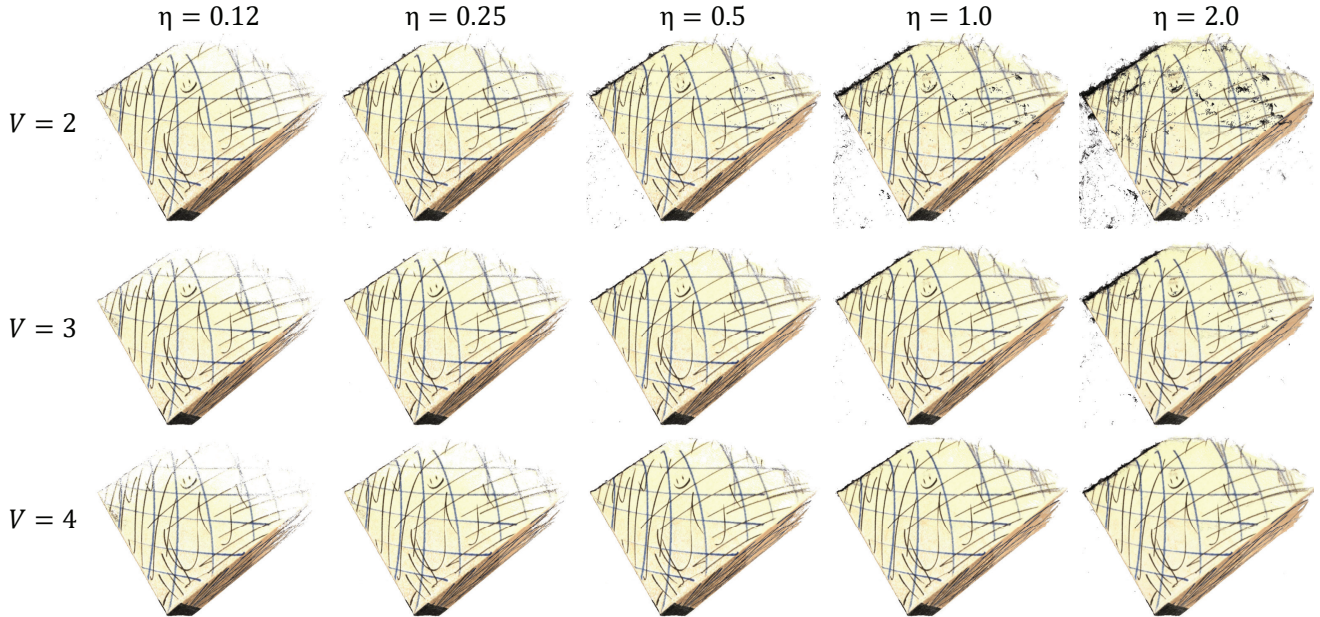


Figure 1: Reconstruction results of *scan10* on the DTU dataset [1] with different fusion parameters.  $\eta$  is the threshold of geometric consistency check.  $V$  is the number of views that a point should be visible. As  $\eta$  increases, the reconstruction becomes denser while has more noise. As  $V$  increases, the reconstruction becomes cleaner while also becomes sparser.

$\eta$	$V$	Acc. (mm)	Comp. (mm)	Overall (mm)
0.12	2	0.3969	0.3140	<b>0.3555</b>
0.12	3	0.3360	0.4030	0.3695
0.12	4	<b>0.3007</b>	0.5212	0.4109
0.25	2	0.4663	0.2843	0.3753
0.25	3	0.3951	0.3341	0.3646
0.25	4	0.3542	0.3959	0.3750
0.5	2	0.5480	<b>0.2773</b>	0.4127
0.5	3	0.4614	0.3076	0.3845
0.5	4	0.4128	0.3447	0.3788
1.0	2	0.6655	0.2888	0.4772
1.0	3	0.5555	0.3091	0.4323
1.0	4	0.4923	0.3330	0.4126
2.0	2	0.8381	0.3187	0.5784
2.0	3	0.7002	0.3323	0.5163
2.0	4	0.6152	0.3500	0.4826

Table 2: Quantitative results of reconstruction quality on the DTU evaluation dataset [1]. Increasing the geometric consistency threshold  $\eta$ , the reconstructed points become less accurate but also become more complete. Increasing the number of visible views  $V$ , the reconstruction becomes accurate while also becomes incomplete.

Table 3, Gauss-Newton refinement can significantly improves the reconstruction quality. However, the performance improvements of applying Gauss-Newton refinement with more iterations are marginal. Therefore, we only use one iteration in Gauss-Newton refinement.

# iterations	Acc. (mm)	Comp. (mm)	Overall (mm)
0	0.3679	0.4475	0.4077
1	<b>0.3360</b>	0.4030	0.3695
2	0.3391	0.3956	0.3673
3	0.3420	0.3902	0.3662
4	0.3435	0.3885	0.3660
5	0.3443	<b>0.3875</b>	<b>0.3659</b>

Table 3: Quantitative results of reconstruction quality on the DTU evaluation dataset [1] with different iteration number in Gauss-Newton refinement.

## 4. Reconstruction results

We show more reconstruction results on the DTU dataset [1] in Figure 2. Our reconstruction is dense and accurate for all scenes.

## References

- [1] Henrik Aanæs, Rasmus Ramsbøl Jensen, George Vogiatzis, Engin Tola, and Anders Bjorholm Dahl. Large-scale data for multiple-view stereopsis. *International Journal of Computer Vision*, pages 1–16, 2016. 2, 3
- [2] Rui Chen, Songfang Han, Jing Xu, and Hao Su. Point-based multi-view stereo network. In *The IEEE International Conference on Computer Vision (ICCV)*, 2019. 1
- [3] Simon Donne and Andreas Geiger. Learning non-volumetric depth fusion using successive reprojections. In *The IEEE Con-*



Figure 2: Reconstruction results on the DTU dataset [1].

*ference on Computer Vision and Pattern Recognition (CVPR)*,  
June 2019. 1

- [4] Yao Yao, Zixin Luo, Shiwei Li, Tian Fang, and Long Quan. Mvsnet: Depth inference for unstructured multi-view stereo. In *Proceedings of the European Conference on Computer Vision (ECCV)*, pages 767–783, 2018. 1